

SCIENTIFIC REPORTS



OPEN

Metabolomics Approach Based on Multivariate Techniques for Blood Transfusion Reactions

Seul Ji Lee¹, Haiping Wang¹, Soo Hyun Ahn², Mi Kwon Son³, Gyu Hwan Hyun¹, Sang Jun Yoon¹, Jeongmi Lee⁴, Jeong Hill Park^{5,6}, Johan Lim⁷, Soon-Sun Hong³ & Sung Won Kwon⁵

Blood transfusions temporarily improve the physical state of the patient but exert widespread effects on immune and non-immune systems. Perioperative allogeneic blood transfusions (ABT) are associated with various risks, including coagulopathy, incompatibility, transmission of infectious agents, and allergic reactions. Nevertheless, little is known about the global metabolic alterations that reflect the possible reactions of blood transfusions. In this study, we investigated metabolite changes generated by ABT in a rat model using metabolomics technology. To further profile the “metabolome” after blood transfusions, we used both liquid chromatography-quadrupole time-of-flight high-definition mass spectrometry and gas chromatography-mass spectrometry. ABT promoted a stimulatory microenvironment associated with a relative increase in glucose transporter 1/4 (GLUT1/GLUT4) expression. Supporting this result, glucose metabolism-related enzyme IRS1 and interleukin-6 (IL-6) were abnormally expressed, and levels of lysophosphatidylcholine (LysoPC) and its related enzyme phospholipase A2 (PLA2) were significantly altered in allogeneic groups compared to those in autologous groups. Finally, amino acid metabolism was also altered following ABT. Taken together, our results show a difference between autologous and allogeneic blood transfusions and demonstrate correlations with cancer-associated metabolic changes. Our data provide endogenous information for a better understanding of blood transfusion reactions.

As a lifesaving therapeutic treatment, there is a need for blood transfusions in patients undergoing surgery¹ or with anemia². However, blood transfusions still pose significant risks, including coagulopathy, incompatibility, transmission of infectious agents, and allergic reactions^{3–7}. In a recent study, although blood transfusion reactions are rare, the risk of death, postoperative infection, and other adverse clinical outcomes was elevated among patients who received perioperative allogeneic blood transfusion (ABT)^{8,9}. Moreover, based on the integration of data from observational studies via meta-analyses, significant associations between perioperative ABT and related cancer-specific mortality or cancer recurrence have been reported^{10,11}. Accordingly, it is worth noting that the situations in which patients are perioperatively given ABT are likely to show side effects or induce cancer recurrence. Although a hypothesis regarding the genome and proteome, termed transfusion-related immunomodulation (TRIM), has been extensively proposed^{12,13}, the molecules and mechanisms involved have not been fully elucidated¹⁴. Additionally, it is not known whether this problem is confined to immunosuppression.

Metabolomics involves the systematic study of endogenous metabolites and aims to comprehensively quantify and identify metabolites from biological samples that are the end products of cellular processes¹⁵. Gene expression data and proteomic analyses cannot provide a full description of the underlying physiology, and thus metabolomics is a useful supplement, offering a better understanding of physiological changes¹⁶. For the sake of gaining new insight into blood transfusions as well as to provide a new theoretical basis for clinical research, it is necessary to clarify the global metabolic alterations that accompany blood transfusions. The exploration of biomarkers

¹College of Pharmacy, Seoul National University, Seoul, 08826, Korea. ²Department of Mathematics, Ajou University, Suwon, 16499, Korea. ³College of Medicine, Inha University, Incheon, 22212, Korea. ⁴School of Pharmacy, Sungkyunkwan University, Suwon, 16419, Korea. ⁵College of Pharmacy and Research Institute of Pharmaceutical Sciences, Seoul National University, Seoul, 08826, Korea. ⁶Faculty of Pharmacy, Ton Duc Thang University, Ho Chi Minh City, Vietnam. ⁷Department of Statistics, Seoul National University, Seoul, 08826, Korea. Correspondence and requests for materials should be addressed to S.-S.H. (email: hongs@inha.ac.kr) or S.W.K. (email: swkwon@snu.ac.kr)

contributes significantly to the development of supporting theoretical explanations for the results of clinical study. Distinguishing allogeneic blood transfusions from autologous blood transfusions may lead to the identification of critical biomarkers with adverse impacts on cancer patients who receive ABT for treatment¹⁷.

As a model for the study of humans, rats offer many advantages over mice and other organisms. More specifically, rats were once successfully used in blood transfusion research^{18–20}. In this article, we established blood transfusion models in two strains of laboratory rats, Lewis rats and Sprague-Dawley (SD) rats, as all members of each strain are nearly genetically identical²¹. Moreover, due to the high sensitivity and selectivity of high performance liquid chromatography-quadrupole-time-of-flight combined with mass spectrometry (HPLC-Q-TOF-MS)²², it is often used to profile changes in endogenous metabolites. Additionally, gas chromatography combined with mass spectrometry (GC-MS) has particular advantages for the analysis of compounds with relatively low molecular weights^{23,24}; therefore, more comprehensive metabolite profiling can be conducted by performing both HPLC-Q-TOF-MS and GC-MS.

This study focused on the differences between autologous and allogeneic blood transfusions in a rat model that provides a highly physiologically relevant setting for studying the interplay between blood transfusions and homeostasis in the microenvironment. The acquired data were optimized using a series of statistical approaches, and differential metabolites were identified using standards and databank-based MS/MS spectrum analysis. On the basis of the relevant literature and pathway databases, the biological natures of the various markers, including lipids, glucose, and amino acids, were discussed to further elucidate the possible mechanisms underlying the negative impact of ABT. We also found that levels of GLUT1/4, PLA2, IL-6, and IRS-1 varied in the plasma. Interestingly, these common transporters or signals differentially affected the regulatory cells involved in cancer metabolism. These findings suggest new non-clinical evidence of blood transfusion-associated impacts on cancer.

Results

Observation. Fourteen Lewis rats received a 1-mL transfusion of Lewis rat blood through the dorsal vein as a control (autologous) group, and 14 others received a 1-mL transfusion with SD rat blood as a test (allogeneic) group. Seven days after autologous blood transfusion and ABT, all of the experimental animals appeared in good condition, and no abnormalities were found. During the process of blood sampling, no hemolysis occurred.

Global detection of biomarker candidates. We used HPLC-Q-TOF-MS and GC-MS to identify global differences in metabolites in rat blood following autologous and allogeneic blood transfusions. We implemented the empirical Bayes procedure by Efron²⁵ [local false discovery rate (FDR)] to control for multiple testing errors that arise when testing many hypotheses simultaneously. At a local FDR level of 0.1, we tested both the null hypothesis (H_{p0}) of no difference in the proportion of subjects with a non-zero intensity and the null hypothesis ($H_{\mu0}$) of no difference in the mean of the intensity. Therefore, we tested the overall null hypothesis ($H_0 = H_{p0} \cap H_{\mu0}$) of no difference in both the proportion and mean of the intensity at a local FDR level of 0.2 ($= 2 \times 0.1$).

More specifically, for the HPLC-Q-TOF-MS data, we considered the i^{th} metabolite as displaying a significantly different non-zero intensity proportion if $p_{pi}^{LC} \leq 5.765 \times 10^{-3}$ at the local FDR level of 0.1. Also, at the local FDR level of 0.1, we considered the i^{th} metabolite as showing a significantly different mean of the intensity if $p_{\mu i}^{LC} \leq 5.969 \times 10^{-7}$. As a result, we identified 474 significant metabolite features at a local FDR level of 0.2 based on the HPLC-Q-TOF-MS data. In the same manner, for the data from GC-MS, we identified 196 metabolite features satisfying $p_{pj}^{GC} \leq 4.846 \times 10^{-2}$ or satisfying $p_{\mu j}^{GC} \leq 6.812 \times 10^{-5}$ at a local FDR level of 0.2.

Identification of differential metabolites. Identification of compounds detected by GC-MS was based on comparisons of mass spectra, retention indices (RIs), and authentic standards. According to comparison with the NIST and WILEY mass spectral databases registered in the GC-MS analysis system, followed by detection of the corresponding standards using GC-MS, 16 metabolites were identified. The combination of chromatographic properties and mass spectra gave an indication of a match to a specific compound (Fig. S4). In HPLC-Q-TOF-MS analysis, structural elucidation of metabolites should be routinely performed by the acquisition of additional MS data. Therefore, in the second step, we applied MS/MS experiments using an ion collision energy of 10–50 eV in the positive mode to obtain structural information via interpretation of the fragmentation patterns of the biomarker candidates. The typical mass error was less than 5 ppm. All lysophosphatidylcholines (LysoPCs) were confirmed based on characteristic fragments of 184.07, 104.11, and 86.1 m/z, as previously described^{26,27}. These features were tentatively compared with those of the online database. The identification results confirmed that most of the candidates had a specific spectrum (Figs S5–S13). To qualitatively evaluate the confidence of metabolite identification, the standard LysoPC(17:0) was run on the same instrument with the same parameters.

Ultimately, 24 discriminant metabolites for distinguishing allogeneic from autologous blood transfusions were identified, including LysoPC (14:0), LysoPC (16:0), LysoPC (16:1), LysoPC (18:0), LysoPC (18:1), LysoPC (18:2), LysoPC (20:2), LysoPC (20:4), alanine, citric acid, glucose, glutamic acid, glutamine, glycine, isoleucine, lactic acid, lysine, ornithine, proline, pyroglutamic acid, serine, threonine, urea, and valine (Table 1).

Multivariate analysis. Principal component analysis (PCA) plots were generated to visualize the explanatory power of the identified marker candidates. The concentrations of the 24 marker candidate metabolites were confirmed to differ depending on the type of transfusion (allogeneic or autologous), as shown by the score plot, and the differences were confirmed by partial least squares discriminant analysis (PLS-DA) (Fig. 1).

Furthermore, clustering analysis was conducted using these 24 marker candidates. Samples from each of the blood transfusion types were shown to cluster as a group (Fig. 2), and a heat map of the clustering results was generated using Euclidian distances and Ward's linkage.

	Potential biomarker	Molecular weight	$-\log_{10}(p)$	Log_2 (Fold change) (test/control)
GC-MS	Alanine	89.09	1.90	-12.49
	Citric acid	192.12	1.86	-3.56
	Glucose	180.16	6.33	1.89
	Glutamic acid	147.13	5.01	15.07
	Glutamine	146.15	19.79	-11.82
	Glycine	75.07	3.02	-2.02
	Isoleucine	131.18	11.32	-11.76
	Lactic acid	90.08	4.17	17.62
	Lysine	146.19	10.44	-15.32
	Ornithine	132.16	1.89	-10.52
	Proline	115.13	5.31	5.19
	Pyroglutamic acid	129.12	1.87	13.72
	Serine	105.09	2.64	2.99
	Threonine	119.12	6.14	17.49
Urea	60.06	2.86	-13.52	
Valine	117.15	3.48	11.92	
HPLC-Q-TOF-MS	LysoPC (14:0)	467.30	22.43	-2.32
	LysoPC (16:0)	495.33	2.56	-1.39
	LysoPC (16:1)	493.32	2.13	-0.94
	LysoPC (18:0)	523.36	3.38	-1.14
	LysoPC (18:1)	521.35	2.02	-1.29
	LysoPC (18:2)	519.33	2.32	-3.16
	LysoPC (20:2)	547.36	4.21	-1.23
	LysoPC (20:4)	543.68	3.47	-5.39

Table 1. Identified metabolites that differentiate rats subjected to allogeneic (test) and autologous (control) blood transfusions.

Sandwich enzyme-linked immunosorbent assay (ELISA). We analyzed IL-6, GLUT1, GLUT4, PLA2, and IRS1 levels in rat sera using sandwich ELISA, and each analysis included a standard curve. A representative standard curve for each of the five analyses is shown in Fig. 3(a–e). The linearity of each standard curve was confirmed, and R values of 0.99 (0.96 for GLUT1) were noted. The GLUT1, GLUT4, and IL-6 levels of the ABT test group were increased by approximately 143%, 116%, and 414%, respectively, compared with levels in the control group. In contrast, levels of PLA2 and IRS1 were approximately 54% and 44% lower than those of the autologous blood transfusion group, indicating the loss of activity of these two receptors (Fig. 3f). All five of these analyses showed significant differences ($p < 0.05$) between the autologous and allogeneic blood transfusion groups.

Pathway analysis and interpretation. We next aimed to evaluate the obtained metabolomes in depth using Ingenuity Pathway Analysis (IPA), a web-based omics application for analyzing and interpreting metabolomes and transcriptomes. The results of pathway analysis showed that each metabolite or protein was directly or indirectly related to the others (Fig. 4). Notably, all 22 entities were found to be connected with the entity “cancer”, indicating that changes in endogenous expression as a result of ABT may be related to cancer. The results of the fold change analysis revealed that the metabolome expression of lysine, urea, alanine, glutamine, isoleucine, ornithine, LysoPC(20:4), citric acid, LysoPC(18:2), LysoPC(14:0), glycine, LysoPC(16:0), LysoPC(18:1), LysoPC(20:2), and LysoPC(18:0) in the allogeneic group was less than half that in the control group. Moreover, the metabolome expression of glucose, serine, proline, valine, pyroglutamic acid, glutamic acid, threonine, and lactic acid in the allogeneic group was more than twice that in the control group. Additionally, we used MetaboAnalyst to conduct an enrichment analysis of this pathway-associated metabolite set. The results indicated a significant Warburg effect ($p = 0.00132$, FDR = 0.0234) (Fig. S14).

Discussion

In this study, we conducted for the first time a metabolic profile of rats undergoing allogeneic and autologous blood transfusions using GC-MS and HPLC-Q-TOF-MS to identify potential metabolic responses. Based on pathway analysis, the identified metabolites and proteins were found to be related to the entity “cancer”, implying a relationship between ABT and cancer.

The modulation of the immune systems of ABT recipients has been accepted as a condition known as TRIM²⁸. As a key component of low-density lipoproteins (LDL)²⁹, LysoPC regulates a variety of biological processes, including cell proliferation, tumor cell invasiveness, and inflammation. Not only does it promote inflammatory effects, including increased expression of endothelial cell adhesion molecules and growth factors, monocyte chemotaxis, and macrophage activation^{30,31}, but it also is considered to be a potent regulator of T cell-activated inflammation at sites of tissue damage based on a previous study. Therefore, LysoPC is a natural adjuvant for the immune system, inducing humoral and cellular immune responses³². As a consequence, the reductions in

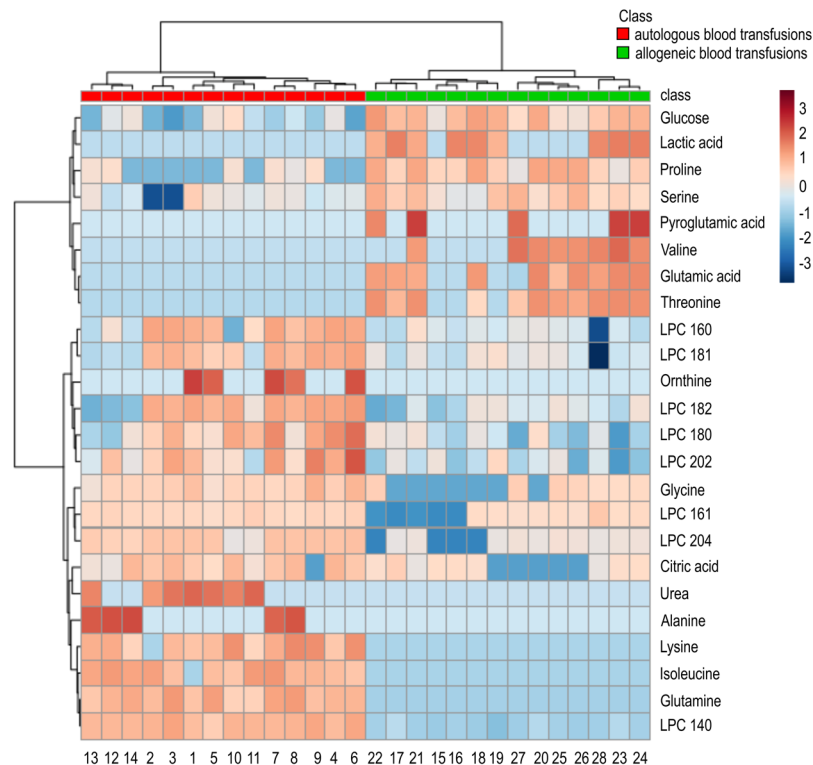


Figure 2. Heat map visualization of 24 significantly altered features in allogeneic (test) blood transfusion samples compared to those in autologous (control) blood transfusions. Shades of red and blue indicate increases and decreases, respectively, in the concentrations of metabolites. Clustering results are also shown. Euclidean distances were measured, and Ward's clustering algorithm was used to construct the heat map.

importance in the metabolic reprogramming of proliferating cells. Many amino acid metabolic enzymes are described as immunosuppressive in the tumor microenvironment and represent targets for cancer therapy⁴⁴. Therefore, it is expected that changes in the expression of these amino acids in the metabolome following ABT would have the potential to affect the development of cancer.

Based on the biomarkers identified in this study, we propose a metabolic pathway related to blood transfusion-induced changes. Our ELISA results help to illustrate the possible roles of different transporters and signaling molecules. The suppression of IRS1 and the activation of IL-6 are both reported to induce or promote tumor metastasis^{45,46}. Although the pathways identified by previous studies^{47–49} indicated, in part, the dysregulation of LysoPC and glucose in some diseases, the elucidation of this pathway will facilitate our understanding of the likely effects of ABT. However, additional studies should be conducted to confirm the role of this pathway in blood transfusions and cancer recurrence.

Methods

Chemicals and reagents. All chemicals and reagents, unless otherwise stated, were purchased from Sigma-Aldrich Inc. (St. Louis, MO, USA). HPLC-grade chloroform, water, acetonitrile, and methanol were purchased from Avantor Performance Materials Inc. (Center Valley, PA, USA). The lipid standard was purchased from Avanti Polar Lipids (Alabaster, AL, USA).

Rat model, blood transfusions, and sample collection. Twenty-eight male adult Lewis rats (160–180 g) were used as the transfusion recipients, while 14 adult Lewis rats and 14SD rats were used as blood donors. All animals were housed in individual cages and given food and water ad libitum throughout the study. Animals were observed for over two weeks prior to initiation of the study to check for evidence of pre-existing abnormalities.

Blood was obtained from donor animals by vena cava puncture and was transfused into recipients immediately after drawing to avoid the influence of anticoagulants and additional agents. Fourteen Lewis rats received a 1-mL transfusion⁵⁰ with Lewis rat blood through the dorsal vein as a control group, and 14 others received a 1-mL transfusion with SD rat blood as a test group. This volume of donor blood was chosen to closely approximate the intravascular volume changes achieved in animals receiving 1 mL of whole blood¹⁹.

Animals were sacrificed 7 days after transfusion via cardiac air embolus. A total of 2 mL whole blood was obtained from each recipient by vena cava puncture through a laparotomy incision. Blood was placed in equal-volume heparin tubes before centrifugation at $1,300 \times g$ and 4°C . Plasma was kept on ice for about 4 h before testing. The remaining samples were stored at -65°C until further analysis.

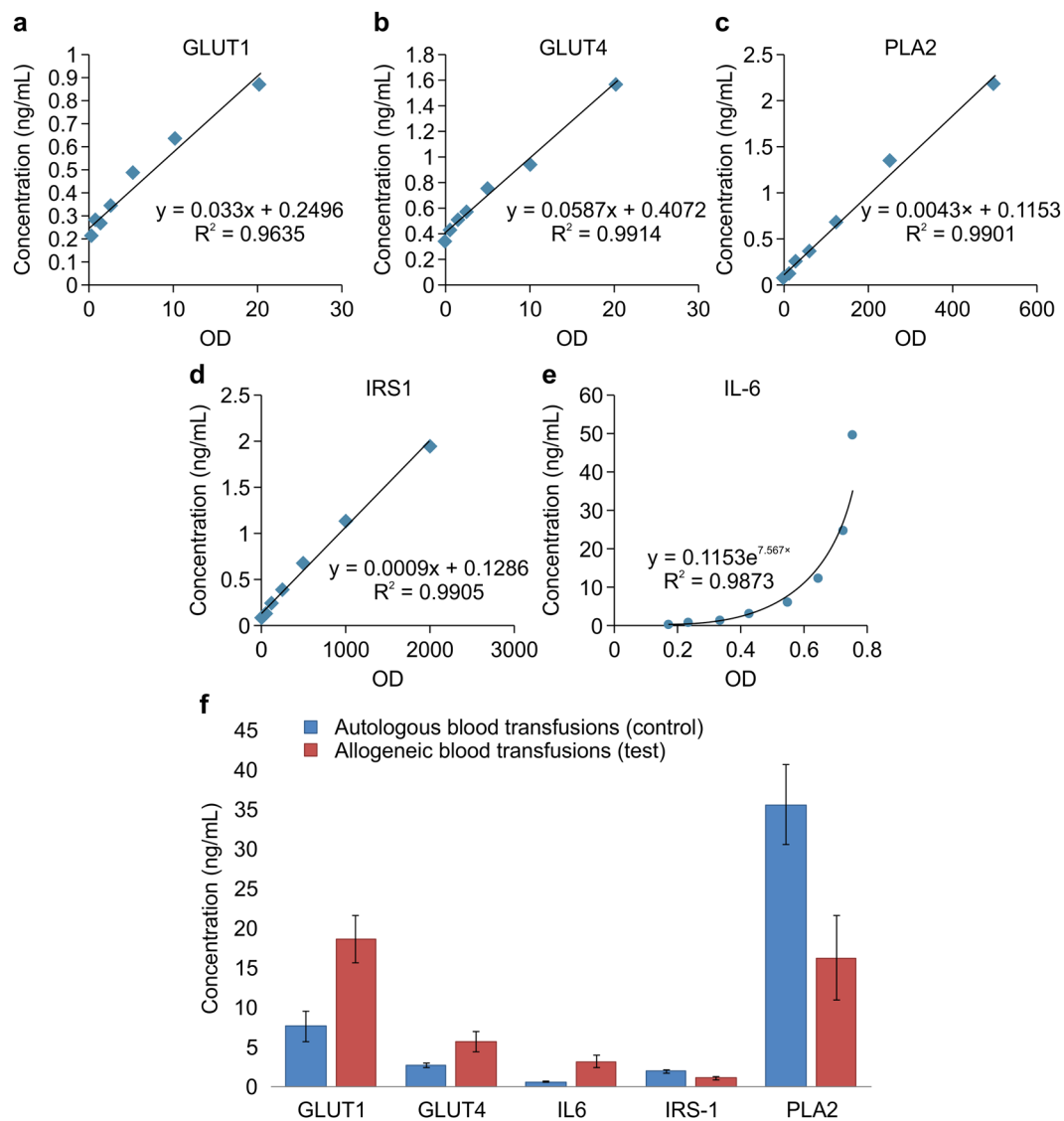


Figure 3. Calibration curves of the typical standards of GLUT1 (a), GLUT4 (b), PLA2 (c), IRS1 (d), and a rat IL-6 ELISA (e, exponential form) kit are shown. The calculated concentrations of the optical densities of GLUT1, GLUT4, PLA2, IRS1, and IL-6 (f) in sera from rats subject to autologous and allogeneic blood transfusions were determined by sandwich ELISA.

All rat experiments were approved and reviewed by Inha University (Approval ID: INHA 140321-283) and were performed in accordance with relevant guidelines and regulations.

Sample preparation. *GC-MS.* To each 100 μ L aliquot of plasma, 250 μ L of solvent with a volume ratio of 2.5:1:1 of methanol, water, and chloroform was added, followed by vortexing for 1 min. After heating at 60°C for 30 min, the sample was centrifuged at 14,000 \times g and 4°C for 5 min⁵¹. A 250- μ L sample of supernatant was transferred to a clean test tube and dried under nitrogen at 20°C. The residue was then oximated with 40 μ L methoxyamine hydrochloride (20 mg/mL in pyridine) and kept at 60°C for 60 min, followed by the addition of 20 μ L *N,O*-bis(trimethylsilyl)trifluoroacetamide-trimethylchlorosilane (BSTFA-TMCS). The mixture was then kept at 60°C for another 45 min and filtered by centrifugation at 14,000 \times g and 20°C for 10 min. The supernatant was collected for injection.

HPLC-Q-TOF-MS. Protein was precipitated with a threefold volume of acetonitrile (final concentration, 25%), followed by vortexing for 2 min and centrifugation at 14,000 \times g and 4°C for 20 min. The supernatant was dried by purging with nitrogen. For analysis, samples were reconstituted in 100 μ L acetonitrile/water (4:1) solvent⁵². Mixtures of pooled test group samples and pooled control group samples in a 1:1 (v:v) ratio with solvent were used as quality control (QC) samples.

GC-MS analysis. GC-MS analysis was performed using a GCMS-QP2010 system (Shimadzu, Germany). Chromatographic separation was performed on a DB-5MS column (30 m \times 0.25 mm, 0.25 μ m, Agilent

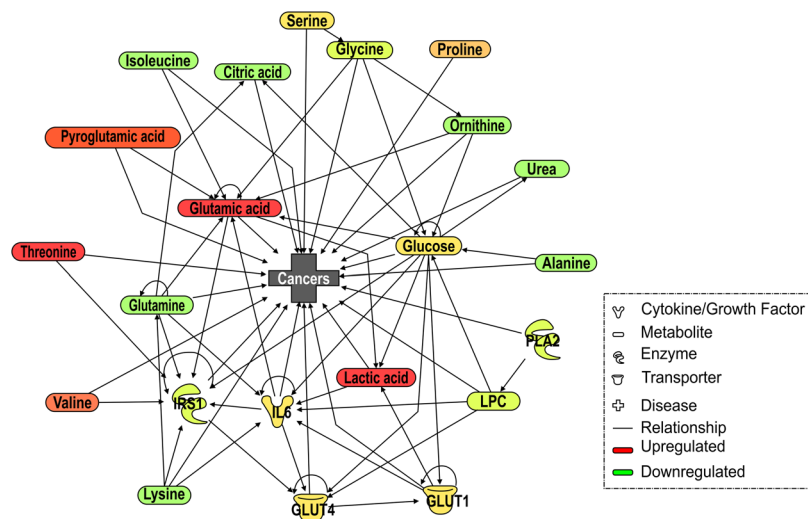


Figure 4. Metabolic pathway analysis of variations induced after ABT by IPA. (QIAGEN Inc., <https://www.qiagenbioinformatics.com/products/ingenuitypathway-analysis>) Up- and downregulated metabolites and those with no change are shown in red, green, and yellow, respectively.

Technologies, Santa Clara, CA, USA). The GC oven temperature was held at 100°C for 5 min, increased to 180°C at a rate of 5°C/min, then increased to 300°C at a rate of 5°C/min and held at the final temperature for 5 min. A 1- μ L sample was injected in the split mode, and helium (99.9999% He) was used as the carrier gas at a constant flow of 1 mL/min. The injection temperature and ion source temperature were 300°C and 200°C, respectively. After a 3-min solvent delay, mass spectra were obtained at 4 scans per second with a mass range of m/z 40–600. The ionization energy was 70 eV in the electron impact mode. Standards were injected for identification.

HPLC-Q-TOF-MS analysis. LC-MS analysis was performed on an HPLC (Agilent) system equipped with an ODS column (100 \times 2.1 mm, 1.7 μ m) and coupled to an electron spray ionization quadrupole TOF-mass spectrometer (6510 ESI-Q-TOF-MS, maXis, Bruker, Billerica, MA, USA). The column temperature was 50°C with a flow rate of 0.35 mL/min. For non-targeted metabolomics, a linear gradient was applied for the first 26 min and then changed from 98% A (0.1% formic acid in water) to 100% B (acetonitrile) by holding for 20 min⁵². The mass spectrometer was operated in the ESI positive ionization mode, with ultra-high purity nitrogen as the nebulizer and drying gases (8.0 L/min) at a temperature of 200°C. The scan mode was applied for detection, and the scan mass ranged from 50 to 1000 m/z . For characterization and

QC data, a QC sample (a mixture of every sample) was injected at regular intervals during the run sequence. To obtain information for the identification of the metabolites, data-dependent MS/MS was performed by a collision energy ramp from 10 to 50 eV. All other parameters were the same as mentioned above. The standard LysoPC(17:0) was chosen to confirm the identification results. The entire process was performed using chromatography software (Bruker Daltonics).

Data processing and statistical analysis. After data acquisition by HPLC-Q-TOF-MS and GC-MS, de-noising, baseline correction, and peak detection were performed. To exclude noise peaks in the subsequent analysis, MZmine 2.10⁵³ (<http://mzmine.github.io/>) was employed for data pre-processing (Fig. S1).

We tested whether there was a significant difference in the intensity of each metabolite between control and treatment groups using R software. Noting that the observed data were derived from only a few samples and frequently had intensity values of zero for each metabolite, we compared not only the mean of the (log-transformed) intensity but also the proportion of detected samples (subjects having a non-zero intensity) for each metabolite between the two groups.

For the i^{th} or j^{th} metabolite, to compare the proportions of detected samples with a small sample size, we used a chi-squared test with continuity correction⁵⁴ and observed the p -values p_{pi}^{LC} based on the data from LC for $i = 1, \dots, 13872$ and p_{pj}^{GC} based on the data from GC for $j = 1, \dots, 6089$. Further, to test the mean difference, we considered an independent two-sample t -test using detected subjects and observed the p -values $p_{\mu i}^{LC}$ and $p_{\mu j}^{GC}$ based on the data from LC and GC, respectively.

Identification of differential metabolites. Using GC-MS data, the selected metabolites were identified against standards, and a metabolite was deemed to be positively identified if the retention time and MS spectrum matched those of the authentic standards. For HPLC-Q-TOF-MS, MS/MS data were analyzed using a recently published strategy for the identification of selected metabolites^{55,56}. Based on the accurate mass information, the Human Metabolome Database (HMDB) (<http://www.hmdb.ca/>), METLIN (<http://metlin.scripps.edu/index.php>), Massbank (www.massbank.jp/), Lipid Maps (<http://www.lipidmaps.org/>), and PubChem Compound (<http://www.ncbi.nlm.nih.gov>) were searched with a mass accuracy tolerance of 5 ppm to generate a list of

mass-matched putative metabolites. MS/MS spectra emphasize neutral losses and product ions, which are characteristic of a metabolite group and allow for discriminating among database hits. The lipid standard LysoPC(17:0) was detected to verify the identification results by a comparison of its mass spectra and chromatographic retention time with those of plasma samples.

Multivariate analysis. We analyzed the identified metabolites using MetaboAnalyst 4.0⁵⁷ (<http://www.metaboanalyst.ca/>). Log transformation was performed to approximate a normal distribution. Data scaling was performed using the “auto scaling” function. As a result, a box plot and kernel density plot were obtained (Figs S2 and 3). The data were summarized by far fewer variables, called scores, which were weighted averages of the original variables. The weighted profiles were called “loadings.” PCA was conducted using the “prcomp” package. The calculation was based on singular value decomposition.

PLS regression is a control method for the extraction of data that predicts class membership (Y) from the linear combination of original variables (X) using multiple regression analysis techniques. A PLS regression was performed using the “pls” function of the R “pls” package. Classification and cross-validation were performed using the corresponding wrapper function in the “caret” package. A permutation test was conducted to evaluate the importance of class distinction. In each permutation, a PLS-DA model between the data (X) and replaced class-label (Y) was constructed using the optimum number of components, which was identified from a cross-validation test against a model based on the original class assignment.

For the agglomerative hierarchical cluster analysis, each sample started in a separate cluster, and an algorithm combined them until all of the samples clustered together. A heat map was created as a visual aid in addition to phylogenetic trees. Hierarchical clustering was conducted using the “hclust” function in the “stat” package.

ELISA. For analysis of IL-6 levels in rat sera, we used ELISA kits (R&D Systems, Minneapolis, MN, USA). The plates were coated with 100 μ L of 2 μ g/mL anti-IL-6 capture monoclonal antibody diluted in phosphate-buffered saline (PBS) for 24 h at room temperature. The plates were washed three times with PBS containing 0.1% Tween-20 and incubated with 100 μ L/well of 1% bovine serum albumin (BSA, Sigma-Aldrich) in PBS for 1 h at room temperature. The rat sera and various concentrations of recombinant IL-6 were incubated overnight at 4°C. The plates were washed three times with PBS containing 0.1% Tween-20 and incubated with 100 μ L/well of 50 ng/mL biotinylated anti-IL-6 detecting antibody for 2 h at room temperature. The plates were then washed and incubated for 30 min with 100 μ L of horseradish peroxidase-conjugated streptavidin (Vector Laboratories, Burlingame, CA, USA). After washing, the 2,2-azino-bis substrate reaction was stopped by adding 50 μ L of 2 N H₂SO₄. The absorbance was measured at 450 nm using a microplate reader. Ten rats were included in each group, and three replicate wells were used for each analysis. The levels of GLUT1, GLUT4, PLA2, and IRS1 in rat sera were also assessed using ELISA kits (Mybiosource, San Diego, CA, USA) according to the manufacturer’s instructions.

Pathway analysis and interpretation. Data were analyzed through the use of IPA (QIAGEN Inc. <https://www.qiagenbioinformatics.com/products/ingenuitypathway-analysis>)⁵⁸. After importing target metabolites and proteins as entities, we searched for diseases or phenotypes with as many connections as possible with the 22 entities. Concentration values were visualized, with shades of red, green, and yellow indicating up- and downregulation and no change, respectively, based on the log₂ fold change in concentration between the allogeneic and autologous blood transfusion groups. We used MetaboAnalyst to conduct an enrichment analysis. Over-representation analysis (ORA) was implemented using the hypergeometric test to evaluate whether a particular metabolite set was represented more than expected by chance within the metabolite list; *p*-values were provided after adjusting for multiple testing.

References

1. Calabrich, A. & Katz, A. Management of anemia in cancer patients. *Future oncology* **7**, 507–517, <https://doi.org/10.2217/fon.11.24> (2011).
2. Vincent, J. *et al.* Anemia and blood transfusion in critically ill patients. *JAMA* **288**, 1499–1507, <https://doi.org/10.1001/jama.288.12.1499> (2002).
3. Vanderlinde, E. S., Heal, J. M. & Blumberg, N. Autologous transfusion. *BMJ* **324**, 772–775, <https://doi.org/10.1136/bmj.324.7340.772> (2002).
4. Murphy, P., Heal, J. M. & Blumberg, N. Infection or suspected infection after hip replacement surgery with autologous or homologous blood transfusions. *Transfusion* **31**, 212–217, <https://doi.org/10.1046/j.1537-2995.1991.31391165169.x> (1991).
5. Waymack, J., Rapien, J., Garnett, D., Tweddell, J. S. & Alexander, J. Effect of transfusion on immune function in a traumatized animal model. *Archives of Surgery* **121**, 50–55, <https://doi.org/10.1001/archsurg.1986.01400010056007> (1986).
6. Maxwell, M. J. & Wilson, M. J. A. Complications of blood transfusion. *Continuing Education in Anaesthesia, Critical Care & Pain* **6**, 225–229, <https://doi.org/10.1093/bjaceaccp/mkl053> (2006).
7. Barrett-Lee, P. J., Bailey, N. P., O’Brien, M. E. & Wager, E. Large-scale UK audit of blood transfusion requirements and anaemia in patients receiving cytotoxic chemotherapy. *British journal of cancer* **82**, 93–97, <https://doi.org/10.1054/bjoc.1999.0883> (2000).
8. Al-Refaie, W. B., Parsons, H. M., Markin, A., Abrams, J. & Habermann, E. B. Blood transfusion and cancer surgery outcomes: a continued reason for concern. *Surgery* **152**, 344–354, <https://doi.org/10.1016/j.surg.2012.06.008> (2012).
9. Vamvakas, E. C. Allogeneic blood transfusion and cancer recurrence: 20 years later. *Transfusion* **54**, 2149–2153, <https://doi.org/10.1111/trf.12689> (2014).
10. Bossola, M., Pacelli, F., Bellantone, R. & Doglietto, G. B. Influence of transfusions on perioperative and long-term outcome in patients following hepatic resection for colorectal metastases. *Annals of surgery* **241**, 381 (2005).
11. Sun, C., Wang, Y., Yao, H. S. & Hu, Z. Q. Allogeneic blood transfusion and the prognosis of gastric cancer patients: systematic review and meta-analysis. *International journal of surgery*, <https://doi.org/10.1016/j.ijssu.2014.11.044> (2014).
12. Cata, J. P., Wang, H., Gottumukkala, V., Reuben, J. & Sessler, D. I. Inflammatory response, immunosuppression, and cancer recurrence after perioperative blood transfusions. *British journal of anaesthesia* **110**, 690–701, <https://doi.org/10.1093/bja/aet068> (2013).
13. Vamvakas, E. C. Pneumonia as a complication of blood product transfusion in the critically ill: transfusion-related immunomodulation (TRIM). *Critical care medicine* **34**, S151–159, <https://doi.org/10.1097/01.CCM.0000214310.70642.8C> (2006).

14. Santin, A. D. *et al.* Effect of blood transfusion during radiotherapy on the immune function of patients with cancer of the uterine cervix: role of interleukin-10. *International journal of radiation oncology, biology, physics* **54**, 1345–1355 (2002).
15. Jordan, K. W. *et al.* Metabolomic characterization of human rectal adenocarcinoma with intact tissue magnetic resonance spectroscopy. *Diseases of the colon and rectum* **52**, 520–525, <https://doi.org/10.1007/DCR.0b013e31819c9a2c> (2009).
16. D'Alessandro, A., Giardina, B., Gevi, F., Timperio, A. M. & Zolla, L. Clinical metabolomics: the next stage of clinical biochemistry. *Blood Transfus* **10**(Suppl 2), s19–24, <https://doi.org/10.2450/2012.0055> (2012).
17. Chen, J. *et al.* Practical approach for the identification and isomer elucidation of biomarkers detected in a metabolomic study for the discovery of individuals at risk for diabetes by integrating the chromatographic and mass spectrometric information. *Analytical chemistry* **80**, 1280–1289, <https://doi.org/10.1021/ac702089h> (2008).
18. Wen-zhou, J. I. A. & Huang Mei-xiong, S. J.-h. Influence of intraoperative blood transfusion on tumor growth in rats. *Chinese Journal of Current Advances in General Surgery* **6** (2008).
19. Waymack, J. P., Gugliuzza, K., Dong, Y. L. & Herndon, D. N. Effect of blood transfusion on immune function. IX. Effect on lymphocyte metabolism. *The Journal of surgical research* **55**, 269–272, <https://doi.org/10.1006/jsre.1993.1139> (1993).
20. Atzil, S. *et al.* Blood transfusion promotes cancer progression: a critical role for aged erythrocytes. *Anesthesiology* **109**, 989–997, <https://doi.org/10.1097/ALN.0b013e31818ddb72> (2008).
21. Green, E. L. Genetics and Probability in Animal Breeding Experiments. *Oxford University Press, New York* (1981).
22. Kofeler, H. C., Fauland, A., Rechberger, G. N. & Trotschmuller, M. Mass spectrometry based lipidomics: an overview of technological platforms. *Metabolites* **2**, 19–38, <https://doi.org/10.3390/metabo2010019> (2012).
23. Dunn, W. B. *et al.* Procedures for large-scale metabolic profiling of serum and plasma using gas chromatography and liquid chromatography coupled to mass spectrometry. *Nat Protoc* **6**, 1060–1083, <https://doi.org/10.1038/nprot.2011.335> (2011).
24. Williams, B. J. *et al.* Amino acid profiling in plant cell cultures: an inter-laboratory comparison of CE-MS and GC-MS. *Electrophoresis* **28**, 1371–1379, <https://doi.org/10.1002/elps.200600609> (2007).
25. Efron, B. Large-scale simultaneous hypothesis testing: The choice of a null hypothesis. *J Am Stat Assoc* **99**, 96–104, <https://doi.org/10.1198/016214504000000089> (2004).
26. Milne, S., Ivanova, P., Forrester, J. & Alex Brown, H. Lipidomics: an analysis of cellular lipids by ESI-MS. *Methods* **39**, 92–103, <https://doi.org/10.1016/j.jymeth.2006.05.014> (2006).
27. Lee, S. J. *et al.* Senescing Human Bone-Marrow-Derived Clonal Mesenchymal Stem Cells Have Altered Lysophospholipid Composition and Functionality. *J Proteome Res* **13**, 1438–1449, <https://doi.org/10.1021/pr400990k> (2014).
28. Palomero-Rodriguez, M. A., Laporta-Baez, Y., Sanchez-Conde, M. P. & Mollinedo, F. Inflammatory response, immunosuppression, and cancer recurrence after perioperative blood transfusion. *British journal of anaesthesia* **112**, 576–577, <https://doi.org/10.1093/bja/aeu024> (2014).
29. Oestvang, J., Anthonsen, M. W. & Johansen, B. LysoPC and PAF Trigger Arachidonic Acid Release by Divergent Signaling Mechanisms in Monocytes. *Journal of lipids* **2011**, 532145, <https://doi.org/10.1155/2011/532145> (2011).
30. Kabarowski, J. H., Zhu, K., Le, L. Q., Witte, O. N. & Xu, Y. Lysophosphatidylcholine as a ligand for the immunoregulatory receptor G2A. *Science* **293**, 702–705, <https://doi.org/10.1126/science.1061781> (2001).
31. Kabarowski, J. H. G2A and LPC: regulatory functions in immunity. *Prostaglandins & other lipid mediators* **89**, 73–81, <https://doi.org/10.1016/j.prostaglandins.2009.04.007> (2009).
32. Perrin-Cocon, L. *et al.* Lysophosphatidylcholine is a natural adjuvant that initiates cellular immune responses. *Vaccine* **24**, 1254–1263, <https://doi.org/10.1016/j.vaccine.2005.09.036> (2006).
33. Vamvakas, E. C. Possible mechanisms of allogeneic blood transfusion-associated postoperative infection. *Transfusion medicine reviews* **16**, 144–160, <https://doi.org/10.1053/tmrv.2002.31463> (2002).
34. Berezina, T. L. *et al.* Influence of storage on red blood cell rheological properties. *The Journal of surgical research* **102**, 6–12, <https://doi.org/10.1006/jsre.2001.6306> (2002).
35. Jensen, L. S. *et al.* Postoperative infection and natural killer cell function following blood transfusion in patients undergoing elective colorectal surgery. *The British journal of surgery* **79**, 513–516 (1992).
36. van Twuyver, E. *et al.* Pretransplantation blood transfusion revisited. *The New England journal of medicine* **325**, 1210–1213, <https://doi.org/10.1056/NEJM199110243251704> (1991).
37. Pearce, E. L., Poffenberger, M. C., Chang, C. H. & Jones, R. G. Fueling immunity: insights into metabolism and lymphocyte function. *Science* **342**, 1242454, <https://doi.org/10.1126/science.1242454> (2013).
38. Lai, I. L. *et al.* Targeting the Warburg effect with a novel glucose transporter inhibitor to overcome gemcitabine resistance in pancreatic cancer cells. *Carcinogenesis* **35**, 2203–2213, <https://doi.org/10.1093/carcin/bgu124> (2014).
39. Nijsten, M. W. & van Dam, G. M. Hypothesis: using the Warburg effect against cancer by reducing glucose and providing lactate. *Medical hypotheses* **73**, 48–51, <https://doi.org/10.1016/j.mehy.2009.01.041> (2009).
40. Soga, T. Cancer metabolism: key players in metabolic reprogramming. *Cancer science* **104**, 275–281, <https://doi.org/10.1111/cas.12085> (2013).
41. Jozwiak, P., Krzeslak, A., Wiczorek, M. & Lipinska, A. Effect of Glucose on GLUT1-Dependent Intracellular Ascorbate Accumulation and Viability of Thyroid Cancer Cells. *Nutrition and cancer*, 1–9, <https://doi.org/10.1080/01635581.2015.1078823> (2015).
42. Soga, T. *et al.* Lysophosphatidylcholine enhances glucose-dependent insulin secretion via an orphan G-protein-coupled receptor. *Biochemical and biophysical research communications* **326**, 744–751, <https://doi.org/10.1016/j.bbrc.2004.11.120> (2005).
43. Ehse, J. A., Lee, S. S., Pederson, R. A. & McIntosh, C. H. A new pathway for glucose-dependent insulinotropic polypeptide (GIP) receptor signaling: evidence for the involvement of phospholipase A2 in GIP-stimulated insulin secretion. *J Biol Chem* **276**, 23667–23673, <https://doi.org/10.1074/jbc.M103023200> (2001).
44. Ananieva, E. Targeting amino acid metabolism in cancer growth and anti-tumor immune response. *World J Biol Chem* **6**, 281–289, <https://doi.org/10.4331/wjbc.v6.i4.281> (2015).
45. Ma, Z. *et al.* Suppression of insulin receptor substrate 1 (IRS-1) promotes mammary tumor metastasis. *Molecular and cellular biology* **26**, 9338–9351, <https://doi.org/10.1128/MCB.01032-06> (2006).
46. Yamashita, S. *et al.* Group II phospholipase A2 in invasive gastric cancer cell line is induced by interleukin 6. *Biochemical and biophysical research communications* **198**, 878–884, <https://doi.org/10.1006/bbrc.1994.1125> (1994).
47. Heasley, L. E. *et al.* Induction of cytosolic phospholipase A2 by oncogenic Ras in human non-small cell lung cancer. *The Journal of biological chemistry* **272**, 14501–14504 (1997).
48. Wood, I. S. & Trayhurn, P. Glucose transporters (GLUT and SGLT): expanded families of sugar transport proteins. *The British journal of nutrition* **89**, 3–9, <https://doi.org/10.1079/BJN2002763> (2003).
49. Louie, S. M., Roberts, L. S. & Nomura, D. K. Mechanisms linking obesity and cancer. *Biochimica et biophysica acta* **1831**, 1499–1508, <https://doi.org/10.1016/j.bbali.2013.02.008> (2013).
50. Diehl, K.-H. *et al.* A good practice guide to the administration of substances and removal of blood, including routes and volumes. *Journal of Applied Toxicology* **21**, 15–23, <https://doi.org/10.1002/jat.727> (2001).
51. Nishiumi, S. *et al.* Serum metabolomics as a novel diagnostic approach for pancreatic cancer. *Metabolomics* **6**, 518–528, <https://doi.org/10.1007/s11306-010-0224-9> (2010).
52. Yin, P. *et al.* Preanalytical aspects and sample quality assessment in metabolomics studies of human blood. *Clinical chemistry* **59**, 833–845, <https://doi.org/10.1373/clinchem.2012.199257> (2013).

53. Pluskal, T., Castillo, S., Villar-Briones, A. & Oresic, M. MZmine 2: modular framework for processing, visualizing, and analyzing mass spectrometry-based molecular profile data. *Bmc Bioinformatics* **11**, 395, <https://doi.org/10.1186/1471-2105-11-395> (2010).
54. Yates, F. Contingency table involving small numbers and the χ^2 test. *Supplement to the Journal of the Royal Statistical Society* **1**, 217–235, <https://doi.org/10.2307/2983604> (1934).
55. Calderon-Santiago, M., Priego-Capote, F. & Luque de Castro, M. D. Enhanced detection and identification in metabolomics by use of LC-MS/MS untargeted analysis in combination with gas-phase fractionation. *Analytical chemistry* **86**, 7558–7565, <https://doi.org/10.1021/ac501353n> (2014).
56. Hu, L., Boos, K. S., Ye, M. & Zou, H. Analysis of the endogenous human serum peptides by on-line extraction with restricted-access material and HPLC-MS/MS identification. *Talanta* **127**, 191–195, <https://doi.org/10.1016/j.talanta.2014.04.011> (2014).
57. Chong, J. *et al.* MetaboAnalyst 4.0: towards more transparent and integrative metabolomics analysis. *Nucleic Acids Res.* <https://doi.org/10.1093/nar/gky310> (2018).
58. Krämer, A., Green, J., Pollard, J. J. & Tugendreich, S. Causal analysis approaches in Ingenuity Pathway Analysis. *Bioinformatics* **30**, 523–530, <https://doi.org/10.1093/bioinformatics/btt703> (2014).

Acknowledgements

This work was supported by Basic Science Research Program through the National Research Foundation of Korea (NRF) funded by the Ministry of Education [grant number NRF-2017R1A6A3A11028026]; the Bio-Synergy Research Project of the Ministry of Science, ICT and Future Planning through the National Research Foundation (NRF-2012M3A9C4048796); the National Research Foundation of Korea (NRF) grant funded by the Korean government (MSIP) (NRF-2018R1A5A2024425). S.W.K. would like to thank H.J.S. for inspiring the experiment.

Author Contributions

Conceived of and designed the experiments: S.J.L., H.W., J.L., J.H.P., J.L., S.S.H. and S.W.K. Performed the experiments: S.J.L., H.W., M.K.S., G.H.H. and S.J.Y. Analyzed the data: S.J.L., H.W. and S.H.A. Wrote the manuscript: S.J.L. and H.W.

Additional Information

Supplementary information accompanies this paper at <https://doi.org/10.1038/s41598-018-37468-9>.

Competing Interests: The authors declare no competing interests.

Publisher's note: Springer Nature remains neutral with regard to jurisdictional claims in published maps and institutional affiliations.



Open Access This article is licensed under a Creative Commons Attribution 4.0 International License, which permits use, sharing, adaptation, distribution and reproduction in any medium or format, as long as you give appropriate credit to the original author(s) and the source, provide a link to the Creative Commons license, and indicate if changes were made. The images or other third party material in this article are included in the article's Creative Commons license, unless indicated otherwise in a credit line to the material. If material is not included in the article's Creative Commons license and your intended use is not permitted by statutory regulation or exceeds the permitted use, you will need to obtain permission directly from the copyright holder. To view a copy of this license, visit <http://creativecommons.org/licenses/by/4.0/>.

© The Author(s) 2019